interaction. Our results are not in agreement with this prediction.

ACKNOWLEDGMENTS

We wish to thank Dr. Schawlow and Mr. H. L. B. Gould of Bell Laboratories for providing us with the Supermendur foil, Dr. G. P. Blewett of Brookhaven National Laboratory for the strong-focusing magnets, and Professor G. Failla of the Radiology Department of Columbia University for the loan of the Y^{90} source. Professor L. J. Hayner was most helpful in letting us use her equipment to measure the *B-H* curve. We also extend our thanks to Mrs. M. Biavati, Mr. H. Fleishman, Mr. L. Gruenberg, and Mr. N. Pudliener for helping us to take data. We particularly want to express our deep appreciation to Dr. F. Dyson and Dr. Luke Yuan for their invaluable help in theory and suggestions regarding the experimental setup.

PHYSICAL REVIEW VOLUME 109, NUMBER 1 JANUARY 1, 1958

Oxygen Differential Neutron Scattering and Phenomenological Nuclear Potentials

J. L. FOWLER AND H. O. COHN
Oak Ridge National Laboratory, Oak Ridge, Tennessee

(Received September 10, 1957)

The neutron differential elastic scattering cross section of O^{16} has been measured at and in the vicinity of the 1-Mev resonance as well as at higher nonresonant energies. A phase-shift analysis of the results gives the $s_{\frac{1}{2}}$, $p_{\frac{1}{2}}$, $p_{\frac{3}{2}}$, and $d_{\frac{3}{2}}$ phase shifts up to 2.4-Mev neutron bombarding energy. The bound single-particle states of O^{17}, as well as the *s*- and *d*-wave phase shifts, determine the parameters of a phenomenological potential well which describes the average interaction of the neutron with the O^{16} core. This potential has a depth around 40–45 Mev, which varies slightly for different single-particle configurations, and has a diffuse boundary with a Thomas-type spin-orbit energy term. It is consistent with the potentials which in other work are found to fit data of much higher mass.

INTRODUCTION

IN recent years, measurements of the differential elastic scattering of neutrons in the region in which resonances occur have been pursued from two different points of view. On one hand, differential cross sections are measured at one or more fixed neutron energies on a number of elements with an energy spread such as to average over many resonances of the compound nucleus. The results are interpreted in terms of the complex potential-well model of the nucleus[1] or in terms of the giant-resonance theory.[2] On the other hand, measurements are made as a function of energy on individual nuclei (usually for low-mass elements) with sufficient energy resolution to resolve the resonances of the compound nucleus. In this case the results are analyzed in terms of resonance theory,[3] and lead to the assignment of resonance parameters to the individual levels.

With the measurements of the latter type, differential cross sections in the Mev range have been obtained for isotopes of elements from Li to Ne.[4] The phase-shift analysis of the data leads to information on potential scattering,[5–19] which, in the case of the zero-spin target nuclei C^{12} and O^{16}, where only one channel spin is involved, can give a unique assignment of the potential-scattering phase shifts. For C^{12} and O^{16} the *s*-wave nonresonance phase shifts can be calculated from static potential wells which also give the correct energy position of the $J=\frac{1}{2}+$ single-particle bound states of the compound nuclei C^{13} and O^{17}.[15] In this paper the scattering of neutrons from O^{16} is discussed and the phase-shift analysis up to 2.4 Mev is made so that one is able to compare the predictions of the simple shell model to most of the single-particle properties of O^{17} from the ground state up to this energy.[16] A somewhat

[1] Feshbach, Porter, and Weisskopf, Phys. Rev. **90**, 166 (1953); **96**, 448 (1954).
[2] Lane, Thomas, and Wigner, Phys. Rev. **98**, 693 (1955).
[3] J. M. Blatt and L. C. Biedenharn, Revs. Modern Phys. **24**, 258 (1952).
[4] D. J. Hughes and R. S. Carter, Brookhaven National Laboratory Report BNL-400, June, 1956 (unpublished).
[5] Baldinger, Huber, and Proctor, Helv. Phys. Acta **25**, 142 (1952).
[6] R. Ricamo, Nuovo cimento **10**, 1607 (1953).
[7] Meier, Scherrer, and Trumpy, Helv. Phys. Acta **27**, 577 (1954).
[8] R. Budde and P. Huber, Helv. Phys. Acta **28**, 49 (1955).
[9] Willard, Bair, and Kington, Phys. Rev. **98**, 669 (1955).
[10] J. L. Fowler and C. H. Johnson, Phys. Rev. **98**, 728 (1955).
[11] A. Okazaki, Phys. Rev. **99**, 55 (1955).
[12] Thomas, Walt, Walton, and Allen, Phys. Rev. **101**, 759 (1956).
[13] Willard, Bair, Kington, and Cohn, Phys. Rev. **101**, 765 (1956).
[14] J. E. Wills, Bull. Am. Phys. Soc. Ser. II, **1**, 175 (1956).
[15] J. L. Fowler and H. O. Cohn, Bull. Am. Phys. Soc. Ser. II, **2**, 32 (1957).
[16] J. L. Fowler and H. O. Cohn, Bull. Am. Phys. Soc. Ser. II, **2**, 286 (1957).
[17] E. Van der Spuy, Nuclear Phys. **1**, 381 (1956).
[18] J. D. Seagrave, Phys. Rev. **92**, 1222 (1953).
[19] P. Huber and E. Baldinger, Helv. Phys. Acta **25**, 435 (1952).

similar analysis[17] in terms of a phenomenological interaction in the case of scattering of neutrons from[18,19] He^4 has been found to give the experimental s, p, and d-wave phase shifts in the energy range 0–10 Mev.

In the course of the present experiment, the differential cross section of Be was determined in the range 0.73 to 2.15 Mev; the results will be reported in a subsequent paper.

EXPERIMENT

The differential elastic scattering cross sections of oxygen and beryllium were measured by the method of detecting neutrons scattered from beryllium oxide and beryllium with a shielded counter.[9,10,20] A tritium gas target bombarded with protons from the 5.5-Mv Van de Graaff[21] served as the neutron source with an energy resolution of ~50 kev full width at half maximum. A propane recoil counter, biased to give an approximately flat response at the energies of the scattered neutrons, served as a detector which was shielded by lithiated paraffin from the direct neutrons in a geometry described in the literature.[9] The samples were $\frac{5}{8}$-in. or $\frac{7}{8}$-in. diameter by $4\frac{1}{2}$-in. long BeO cylinders, and metallic Be cylinders of the same length having the same number of Be nuclei as the BeO samples. A number of runs were made at each of the ten angles with the BeO sample, with the Be sample, and with no sample. The background counts from the no-sample runs amounted to approximately the same as the actual counts due to neutrons being scattered from the BeO cylinders.

For the oxygen data, the absolute cross-section scale could be established by several methods: (a) the counter could be calibrated with the same neutrons used for the scattering experiment[9,10] and the differential cross section could be calculated from these data and from a knowledge of the geometry and the weight of the samples; (b) the calibration constant could be obtained from the Be data normalized to the Be total cross section[22] corrected for the Be(n,α) and the Be$(n,2n)$ reactions; or (c) the oxygen data could be normalized independently to the oxygen total cross section.[22–24] Within the errors of the measurements, the three methods gave the same results. At 0.73, 1.50, 1.75, and 2.15 Mev the plotted experimental points in Figs. 1 and 2 are normalized to the oxygen total cross section.[22] For the distributions at the 1-Mev resonance and at 1.21 Mev, Fig. 1, the absolute cross-section scale for the plotted data was obtained from the normalized Be data.

The measured angular distributions were corrected for angular resolution and for the propane counter response where necessary.[9,10] For the measurements at energies above narrow resonances, or far removed from resonances, the multiple-scattering corrections were made by the method of Walt and Barschall.[20] At the 1.00-Mev resonance and at 1.21 Mev, the multiple-scattering correction took into account the effect of variation in the differential cross section for the scattered neutrons degraded in energy. For purposes of calculation, the samples were considered divided into quadrants and the attenuation of the incident and scattered neutrons was found for each quadrant. With the samples used, except at 1.00-Mev resonance, the multiple-scattering correction was less than 8%. At 1.00 Mev this correction amounted to as much as 33%. The uncertainty in the multiple-scattering correction was estimated to be about 30%, so that errors at each point were increased statistically by $\frac{1}{3}$ this correction. Errors shown in the figures are otherwise due to counting statistics.

O^{16} Scattering and Phase Shift Analysis

In Figs. 1 and 2 on the left-hand side, the measured differential cross section of oxygen in the center-of-mass system is plotted against the cosine of the center-of-mass angle. On the right-hand side of the figure is a curve of the total cross section of oxygen taken from the literature.[22] The s resonance which shows up as a dip at 2.37

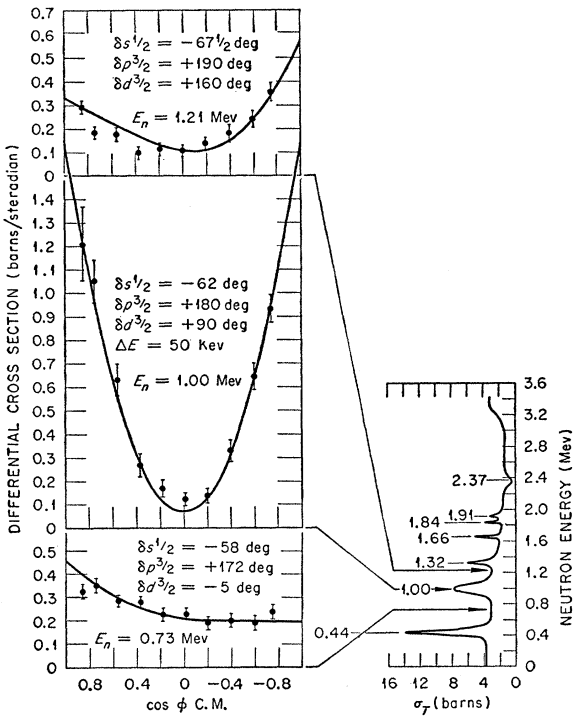

FIG. 1. Differential cross section in the center-of-mass system for scattering of neutrons by oxygen at 0.73, 1.00, and 1.21 Mev. The total cross section of oxygen taken from the literature, reference 22, is given on the right-hand side and connecting arrows indicate the neutron energy for each distribution. The solid theoretical curves are calculated with the set of phase shifts given beside each curve.

[20] M. Walt and H. H. Barschall, Phys. Rev. **93**, 1062 (1954).
[21] Kington, Bair, Cohn, and Willard, Phys. Rev. **99**, 1393 (1955).
[22] Bockelman, Miller, Adair, and Barschall, Phys. Rev. **84**, 69 (1951).
[23] C. K. Bockelman, Phys. Rev. **80**, 1011 (1950).
[24] Frier, Fulk, Lampi, and Williams, Phys. Rev. **78**, 508 (1950).

Mev indicates that the s-wave potential phase shift is about 90° at this energy. Arrows indicate the energy at which the differential cross sections on the left-hand side were measured. The curves are theoretical fits to the data; the phase shifts required are given beside each curve. Knowledge of the angular momentum[22] and parity assignments of the levels,[25] as well as the phase-shift analysis below 700 kev,[11] limits the possibilities and greatly simplifies the process of finding a set of phase shifts to reproduce the experimental data. A change of any phase shift by 5° gives an appreciably worse fit to the data.

In Fig. 3, the phase shifts given in the last figures, as well as other values reported in the literature,[11,22] are plotted against neutron energy. For the $p_{\frac{3}{2}}$ and the $d_{\frac{3}{2}}$ phase shifts, the curves go through 90° or 270° at resonance energies with a slope given by the width of the resonance.[22] Within ±5° the $p_{\frac{1}{2}}$ phase shift is 0 up to 1.75 Mev as Okazaki has observed below 700 kev.[11] The $p_{\frac{1}{2}}$ level at 1.91 Mev[22] contributes a small $p_{\frac{1}{2}}$ phase shift at 2.15 Mev. The uncertainty of the s-wave phase shift, the sine of which is larger than that of the other phase shifts except near resonances, is determined primarily by that of the total cross section.

Single-Particle States of O^{17}

Since O^{16} is a doubly closed shell nucleus, many of the properties of its interaction with nucleons should be describable as if the O^{16} core behaved as an average potential. In other words, much of the information on scattering and bound states involving O^{16} and a neutron can be discussed in the framework of the single-particle

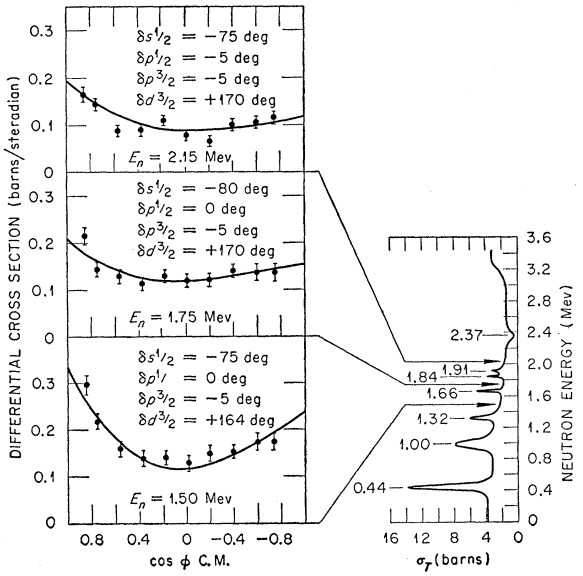

FIG. 2. An extension of the differential cross-section curves described in Fig. 1 to 2.15 Mev.

[25] R. K. Adair, Phys. Rev. **92**, 1491 (1953).

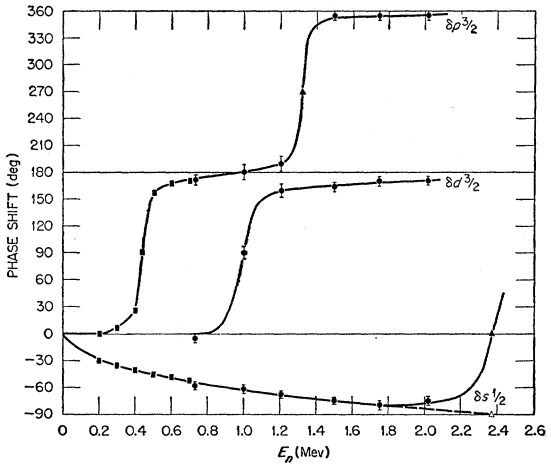

FIG. 3. Experimental phase shifts for neutron scattering from oxygen as a function of neutron energy. Points designated by solid squares from Okazaki,[11] triangular points from total cross section, reference 22. Points designated by circles from present work.

picture. Under the usual assumption that the levels in O^{17} with very large reduced widths are essentially single-particle levels, this information includes: ground state with $J=\frac{5}{2}+$ at −4.14 Mev, below the state of O^{16} and a free neutron, the first excited state with $J=\frac{1}{2}+$ at −3.27 Mev, and an unbound $J=\frac{3}{2}+$ state at 1.00-Mev neutron bombarding energy.[26] The s-wave potential scattering for neutrons also is given in terms of the single-particle picture.

It is simplest to start with s-waves. The $J=\frac{1}{2}+$ level in O^{17} at −3.27 Mev is interpreted as a $2s$-state; the $1s$-states are already filled in the O^{16} core. As a first approximation, consider a square-well potential as giving the average interaction of the core on the neutron. If it is required that this average potential, which describes the elastic scattering data, also give the correct energy of the $2s$ bound state, for a square well only one set of parameters is possible. A well 35 Mev deep and 4.2×10^{-13} cm in radius fits the requirements. For the case discussed here, the complex part of the potential,[1] which in the optical model corresponds to absorption of the nucleon from the single-particle motion, is neglected. In the first place elastic scattering is effectively the only channel open, and in the second place compound elastic scattering for the s and d states discussed here is expected to be very small, since in the energy region considered there are very few compound-nucleus states with even parity and with $\frac{1}{2}$ or $\frac{3}{2}$ units of angular momentum in which the neutron can spend time before it is re-emitted as an elastically scattered particle.

In Fig. 4(b), the experimental s-wave phase shifts from Fig. 3 are replotted, and compared with the phase shift calculated from the square well shown as a dashed

[26] F. Ajzenberg and T. Lauritsen, Revs. Modern Phys. **27**, 77 (1955).

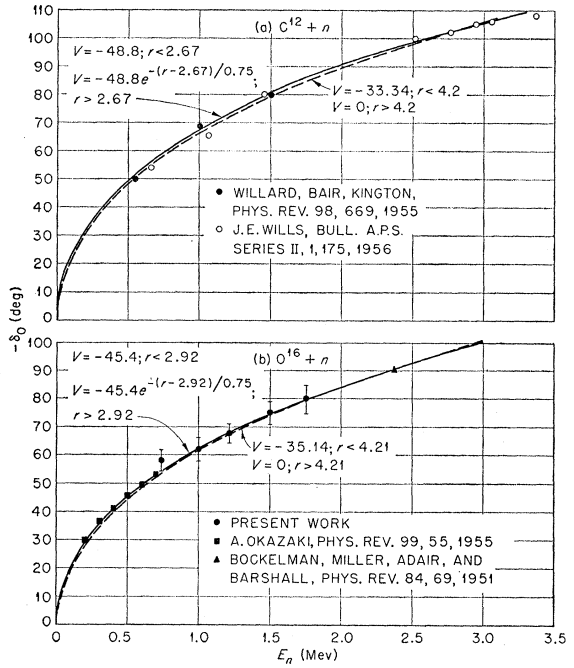

FIG. 4. s-wave phase shifts for neutrons scattered from carbon (a) and oxygen (b) as a function of neutron energy. Curves are calculated from theory based on the potential wells indicated beside each curve. Distances given in the labels are in 10^{-13} cm, and potentials are in Mev.

curve. This curve, which was determined by the s-wave phase shift at $+2.37$ Mev and the energy position of the bound state at -3.27 Mev, agrees satisfactorily with the rest of the s-wave scattering phase shifts. As indicated in Fig. 4(a), the case of C^{12} with the corresponding bound state at -1.86 Mev[26] requires a well 33.3 Mev deep and 4.2×10^{-13} cm in radius to fit both the bound state and the elastic scattering data.[9,14] Since it seemed unreasonable for O and C to have the same radius, the case of a well with a diffuse boundary was investigated. Potential wells with exponential boundaries were used because the bound states in such cases are published in the literature.[27,28] With an exponential tail which falls off with a $1/e$ distance of 0.75×10^{-13} cm as indicated above each solid curve, the phase-shift data are fitted equally well and furthermore the central constant region of the potential varies as $A^{\frac{1}{3}}$.[15]

In calculating the s-wave phase shifts, the exponential well was approximated by a well having 6 steps such that for each step the well strength,[28]

$$\left[S_i=\int_{r_i}^{r_{i+1}} V(r)rdr\right],$$

is the same as it is for the corresponding interval in the exponential well. Similar calculations with a 4-step well give about the same result and indicate that the step approximation is reasonably accurate.

The potential wells should also give the d-states; both the $d_{\frac{5}{2}}$ ground state at -4.14 Mev and the $d_{\frac{3}{2}}$ phase shifts. A spin-orbit energy term is taken in the usual Thomas form,[29]

$$-\frac{\gamma\hbar^2}{2m^2c^2}\frac{1}{r}\frac{\partial V}{\partial r}\left(\frac{\mathbf{l}\cdot\mathbf{s}}{\hbar^2}\right),$$

where γ is an adjustable constant which, from analysis of data in the high mass region, is expected to be ~50.[30,31] For calculating d-wave phase shifts, the wave function was determined in three separate regions and joined at the boundaries by the usual procedure of matching logarithmic derivatives. In the central core region, the solution is the spherical Bessel function. In the external region where the effect of nuclear potential is negligible, the solution is a linear combination of spherical Bessel functions and spherical Neumann functions. In the intermediate region the solution was reduced to the 0 angular momentum case by incorporating the angular momentum term into the potential and the resulting potential well approximated by steps as in the s-wave case discussed above.

With the potential well used for the solid line of Fig. 4(b) and with a spin-orbit term,

$$U_{\mathbf{l}\cdot\mathbf{s}}=+1.18\times10^{-26}\frac{1}{r}\frac{\partial V}{\partial r}\frac{(l+1)}{2}$$

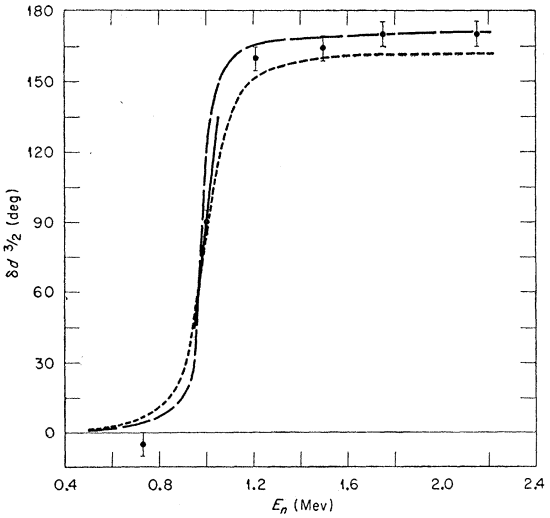

FIG. 5. $d_{\frac{3}{2}}$ phase shift as a function of neutron energy. The slope of the solid line is given by the experimental width of the 1.00-Mev $d_{\frac{3}{2}}$ resonance. The dashed curve is calculated from a potential well having a boundary with a $1/e$ distance of 0.75×10^{-13} cm. For the dotted curve, the $1/e$ distance is 1.00×10^{-13} cm.

[27] A. E. S. Green and Kiuck Lee, Phys. Rev. **99**, 772 (1955).
[28] A. E. S. Green, Phys. Rev. **102**, 1325 (1956).
[29] L. H. Thomas, Nature **117**, 514 (1926); D. R. Inglis, Phys. Rev. **50**, 783 (1936).
[30] Ross, Mark, and Lawson, Phys. Rev. **102**, 1613 (1956).
[31] A. E. S. Green, Phys. Rev. **104**, 1617 (1956).

[$l=2$ for d-waves, and $\gamma\hbar^2/2m^2c^2=1.18\times10^{-26}$ cm^2, or $\gamma=54$], one calculates the dashed curve in Fig. 5. The experimental $d_{\frac{3}{2}}$ phase shifts from Fig. 3 are replotted against energy. The potential with diffuseness parameter of 0.75×10^{-13} cm gives too narrow a width for the $d_{\frac{3}{2}}$ resonance and, as will be seen further on, gives the $d_{\frac{5}{2}}$ bound state at too low an energy.

Increasing the boundary diffuseness improves both situations. Because the bound states have been investigated with spin-orbit energy for a diffuseness parameter of 1×10^{-13} cm,[31] a well with an exponential falloff of 1×10^{-13} cm was tried.

The s-wave data are fitted with a potential:

$$V=-44.2 \text{ Mev}; \quad r<2.76\times10^{-13} \text{ cm},$$

$$V=-44.2\exp\left[-\frac{r-(2.76\times10^{-13})}{1\times10^{-13}}\right]; r>2.76\times10^{-13} \text{ cm}.$$

The calculated s-wave phase-shift curve is indistinguishable from the solid curve in Fig. 4 (b). This potential well, together with a Thomas spin-orbit energy term with $\gamma=45$, gives the $d_{\frac{3}{2}}$ phase shifts similar to the dotted curve in Fig. 5. Under these conditions, the $d_{\frac{5}{2}}$ bound state comes between -7 to -8 Mev.[31] One can, of course, solve the problem for the $d_{\frac{3}{2}}$ states in the case of a square well which gives the s-wave information by introducing a delta-function form for the spin-orbit term. As expected, the calculated width of the $d_{\frac{3}{2}}$ resonance in this case is even narrower than that found in the case of the diffuseness parameter $=0.75\times10^{-13}$ cm and the $d_{\frac{5}{2}}$ bound state comes very low in energy, ~-28 Mev.

Using the square-well and the diffuse-well information, one estimates the diffuseness required to fit the s-wave data and the energy positions of $d_{\frac{5}{2}}$ and $d_{\frac{3}{2}}$ states as about 15% greater than that given by the $1/e$ diffuseness distance of 1×10^{-13} cm. The $d_{\frac{3}{2}}$ phase-shift information in Fig. 5, however, suggests a $1/e$ distance between 0.75×10^{-13} cm and 1.00×10^{-13} cm, in which case the bound state would occur around -10 Mev.

These differences can be reconciled by introducing a slight change in average well depth for the d-wave neutron single-particle configurations, compared to that for the s configuration.[32] This corresponds in a certain sense to a velocity dependence of the potential. For the dotted curve in Fig. 5, which gives the $d_{\frac{3}{2}}$ phase shifts, the well depth was increased from the -44.2 Mev used for the s-states to a depth of -41.2 Mev. This potential then gives the correct energy splitting of the d-states; that is, it gives the energy of the $d_{\frac{5}{2}}$ state correctly. In this case, the constant γ multiplying the spin-orbit term is 35. Since the unsplit $1d$ states are ~3 Mev above the $2s$ state, this change of potential depth corresponds to roughly one Mev per Mev change of neutron energy, which is somewhat higher than the value of 0.5 Mev increase in well depth per Mev change in energy obtained from considerations of nuclei of higher mass.[33,34] A reduction of the $1/e$ distance describing the boundary diffuseness to 0.9×10^{-13} to give a better fit to the width of the $d_{\frac{3}{2}}$ level would require a still larger change in the well depth for the s and d configurations in order to give the correct spin-orbit splitting of the $1d$ states.

In summary, it appears that several bound states and much of the differential elastic scattering data arising from the interaction of a neutron with the closed shell nucleus, O^{16}, can be explained reasonably in terms of an average potential which describes this interaction. This potential as established by the experimental information is a well 40–45 Mev deep which varies slightly for different single-particle configurations. Its diffuse boundary extends about 2.2×10^{-13} cm between the regions which are 90% and 10% of the central well depth. Spin-orbit energy, taken proportional to the derivative of the potential divided by the radius, is approximately 35 times the Thomas term. These properties are consistent with the average phenomenological potentials which have been found to apply for nucleon-nucleus interaction in the region of much higher mass.[30,31,34]

ACKNOWLEDGMENTS

We would like to acknowledge the enlightening discussions of this problem with Dr. A. E. S. Green of Florida State University and Dr. K. A. Brueckner of the University of Pennsylvania. We also thank Dr. H. B. Willard and J. K. Bair for loaning much of the equipment used in the experiment.

[32] We are indebted to Professor K. A. Brueckner for this suggestion.

[33] Brueckner, Eden, and Francis, Phys. Rev. **100**, 891 (1955).
[34] Ross, Lawson, and Mark, Phys. Rev. **104**, 401 (1956).